Article

A Dual Electrochemiluminescence Signal System for In-Situ and Simultaneous Evaluation of Multiple Cell-Surface Receptors

Bin Zhou, Youyi Qiu, Qingqing Wen, Mingyao Zhu, and Peihui Yang

ACS Appl. Mater. Interfaces, **Just Accepted Manuscript** • DOI: 10.1021/acsami.6b12411 • Publication Date (Web): 28 Dec 2016

A Dual Electrochemiluminescence Signal System for In-Situ and Simultaneous Evaluation of Multiple Cell-Surface Receptors

Bin Zhou,[†] Youyi Qiu,[†] Qingqing Wen,[†] Mingyao Zhu,[†] and Peihui Yang,*[,†]

[†]Department of Chemistry, Jinan University Guangzhou 510632, PR China

Corresponding author:
Peihui Yang, Ph.D, Professor
Department of Chemistry, Jinan University
Guangzhou 510632, PR China
E-mail: typhjinan@126.com
Tel/Fax: +86-20-85223039

Abstract: A mutiplex cytosensor based on a dual electrochemiluminescence (ECL) signal system was fabricated for in-situ and simultaneous detection of the expression levels of multiple

cell-surface receptors, mannose and epidermal growth factor receptor (EGFR), using luminol-capped gold nanoparticles (Au@luminol) and CdS quantum dots (CdS QDs) as potential-resolved ECL nanoprobes. Two spatially-resolved areas on indium tin oxides (ITO) electrode were modified with polyaniline (PANI) by electropolymerization, on which gold nanoparticles (AuNPs) were attached to strengthen conductivity and stability of sensing interface. Human mucin1 protein (MUC1) aptamer was immobilized onto AuNPs for capturing MUC1-positive MCF-7 cells. Au@luminol and CdS QDs as ECL nanoprobes were covalently linked with concanavalin A (ConA) and epidermal growth factor (EGF) to label MCF-7 cells on the two areas of the cytosensor separately. Compared to conventional multiplex biosensor, we demonstrated a novel analysis platform for simultaneous detection of multiple cell-surface receptors, it could provide two sensitive and potential-resolved ECL signals during one potential scanning and avoid cross-reactivity between the two nanoprobes. The quantification of MCF-7 cells on the two spatially-resolved areas could be achieved over the linear range from 100 to 1.0×10^6 cells mL^{-1} with a detection limit of 20 cells mL^{-1}. This multiplex cytosensor was further applied for simultaneous quantitative evaluation of the expression levels of mannose and EGFR on MCF-7 cells, revealed that the average numbers of mannose and EGFR per captured MCF-7 cell were 1.2×10^6 and 0.86×10^5 with the relative standard deviation of 5.3 % and 4.2 %, respectively. The multiplex cytosensor was capable of evaluating multiple cell-surface receptors, which would be benefit to develop a better diagnostic tool for diseases.

Keywords: Dual signal system; Multiplex cytosensor; Cell-surface receptors; Mannose; Epidermal growth factor receptor

1. Introduction

Cell-surface receptors exert their numerous physiological roles in regulating various cellular processes, and their dysfunction results in many pathological conditions, especially cancers.[1] The

occurrence of cancer is a complex pattern, which associates closely with the mutation or abnormal expression of multiple cell-surface receptors.[2,3] Mannose, as a member of carbohydrates on cell surfaces, plays important roles in cellular adhesion, immune response and pathological processes.[4] High level of mannose is widespread in the cell surfaces of cancer cells in comparison to normal cells.[5] Moreover, De Leoz et al. deemed that monitoring changes in mannose levels in the onset and progression of cancer can serve as a more specific and sensitive cancer marker.[6] Epidermal growth factor receptor (EGFR) which belongs to the ErbB family of receptor tyrosine kinases (RTK) is involved in the occurrence and progression of cancer and often over-expressed on cancer cells, and both in vivo and in vitro studies have proved that EGFR is capable of inducing cell transformation.[7] The correlation between EGFR overexpression and tumors have been confirmed by many literatures, and highlighting EGFR as a target in cancer therapy.[8,9] It was agreed that simultaneous determination of multiple receptors on cell surface played a crucial role in effective diagnosis of disease.[10–12] Therefore, to develop new methods for simultaneous detecting multiple cell-surface receptors is necessary and will be very important for the research on cancer process.

The traditional biology approaches to analyze biomolecules on cell surface include western blot,[13] fluorescence immunoassay,[14] flow cytometry[15] and so on. Although these methods could offer relative abundance or distribution of biomolecules, most required expensive equipment, chromophores/fluorophores tagging, and mass samples. Currently, electrochemiluminescence (ECL) as a new technique of electrochemistry has been widely applied in bioassay due to its simplicity, high sensitivity, low cost and less sample. So far, most of these established reports just performed single-analyte assays.[16–20] Since pathogenesis is an intricate process and vast majority of diseases have multiple markers associated with their incidence, the assay of single marker is already not adequate to diagnose disease.[10] To satisfy the demands of clinical analysis and disease diagnosis, developing new ECL strategies for multiplex detection of disease markers increasingly attract the attention of researchers.[10–12] Guo et al. fabricated a multiplex ECL immunoassay for detecting CEA and alpha-fetoprotein (AFP) using multicolor quantum dots as label.[10] Feng et al. designed an ECL immunosensor array to perform multiplexed assay of CEA and carbohydrate antigen-199 by using $Ru(bpy)_3^{2+}$-Silica@Poly-L-lysine-Au nanoprobe.[11] Wu et al. developed an ECL imaging mode based on a closed bipolar electrode array to detect multiple cancer biomarkers.[12] Besides, zhang et al. also proposed two multi-signal ECL platforms for

determination of multiple metal ions.[21–22] However, there were few reports dealing with analysis of multiple cell-surface markers, which might owing to the lack of potential-resolved ECL probes and the occur of cross-reactivity among different ECL probes. Han et al. constructed a multiplex immunosensor for determination of cell surface CEA and AFP using $Ru(bpy)_3^{2+}$ and luminol as ECL probes, in which weak ECL signal from luminol at negative potential was quenched by concentrated luminol to obtain two potential-resolved ECL signals from $Ru(bpy)_3^{2+}$ and luminal.[23] Wu et al. described a microchip device with spatially-resolved electrode array for assay of CEA, AFP, and prostate specific antigen on cell surface,[24] which allowed an independent test to be proceed at each electrode for avoiding interference between ECL probes. These methods offered some new strategies to solve the cross-reactivity in multiplex detection. It is reported that the cross-reactivity between different ECL probes might happened if the probes were positioned within the nanometer scale.[23,25-27] In view of this, we designed a more facile device based on ITO electrode with two spatially-resolved areas spaced 3 mm apart, which was much more than the nanometer scale, to exclude the interference between ECL probes. Until now, there is no report concern about simultaneous quantitative evaluation of mannose and EGFR on cell surface. Therefore, it is still a challenge to develop some novel, facile and sensitive ECL strategies for simultaneous evaluation of multiple cell-surface receptors, which is helpful to enhance the diagnosis efficiency of clinical disease.

The application of nanomaterials endowed the various biosensors with excellent property, such as biomolecules immobilization, signal amplification, stability improvement and so forth. Polyaniline (PANI) nanofibers, which has a series of advantage of many microgaps structure, large specific surface and high conductivity, has been widely applied to construct substrate of biosensor.[28,29] Gold nanoparticles (AuNPs) is used extensively to amplify ECL detection signal through improve the loading capacity of biomolecules.[30] Herein, human mucin1 protein (MUC1) aptamer was able to adsorb on the surface of AuNPs via Au-N linkers to functionalize sensing interface for capturing MUC1-positive cells.[31,32] In addition, luminol was attached onto AuNPs (Au@luminol) to form a nanoprobe that amplified ECL signal for labeling cell-surface receptor. L-cysteine-capped CdS QDs was prepared as another ECL nanoprobe combined with the excellent ECL property and the convenient bioconjugation feature. The two nanoprobes could emit ECL signals at positive and negative potentials separately to realize potential-resolved simultaneous

detection.[29,33,34]

Herein, a mutiplex cytosensor based on a dual ECL signal system was first fabricated for simultaneous and in-situ evaluation of the expression levels of mannose and EGFR on MCF-7 cell surface. Two spatially-resolved areas of indium tin oxides (ITO) electrode was electropolymerized with PANI to attach AuNPs for loading MUC1 aptamer. MUC1 aptamer-functionalized sensing interface was used to capture MUC1-positive MCF-7 cells through specific binding of aptamer to ligand. Au@luminol and CdS QDs as ECL nanoprobes were covalently linked with concanavalin A (ConA) and epidermal growth factor (EGF) to label MCF-7 cells on the two spatially-resolved areas of the cytosensor separately, which could prevent the cross-reactivity between the two ECL nanoprobes. The dual ECL signal system exhibited two potential-resolved ECL emissions, and the ECL signal intensity depended on cell amount and mannose and EGFR expression levels at the MCF-7 cell surface. Thus, the ECL cytosensor could be used to detect MCF-7 cells number, and further quantitative evaluation of multiple cell-surface receptors. The proposed cytosensor provided a promising protocol for simultaneous, sensitive and in-situ analysis of multiple disease biomarkers on cell surface.

2. Experimental

2.1. Materials

EGFR was achieved from Sino Biological Inc. (Beijing, China). EGF was obtained from PeproTech Co. Fetal bovine serum (FBS), mannose, concanavalin A (ConA), and bovine serum albumin (BSA) were bought from Sigma-Aldrich (USA). MUC1 aptamer: NH_2-GCAGTTGATCCTTTGGATACCCTGG was obtained from Sangon Biotech (Shanghai) Co., Ltd. MCF-7 cells and human embryonic kidney (HEK) cells were donated by the University of Jinan School of Medicine. DMEM medium was obtained from Gibco Co. ITO electrode (resistance < 7 Ω sq^{-1}) was provided by Zhuhai Kaivo Electronic Components Co. (Shenzhen, China).

2.2. Preparation of ECL nanoprobes

Add 1 mM 3-Mercaptopropionic acid (3-MPA) to as-prepared AuNPs solution, which was stirred for 6 h at 37 °C and then centrifuged (11000 rpm, 25 min) to obtain AuNPs-MPA.

Afterwards, 15 mM N-hydroxysuccinimide (NHS) and 75 mM ethyl(dimethylaminopropyl) carbodiimide (EDC) were added AuNPs-MPA solution to activate carboxylic groups in AuNPs-MPA (37 °C, 1.5 h). Subsequently, 0.5 mL of luminol (0.2 M) solution was applied on AuNPs-MPA in the dark for 12 h. The untreated reagent was removed through dialysis with ultrapure water to obtain luminol-capped AuNPs (Au@luminol). Finally, 0.5 mL of ConA (20 μmol L^{-1}) solution was added in activated Au@luminol solution and subsequently incubation at 4 °C for 4 h. The obtained Au@luminol-ConA was re-suspended with PBS buffer (0.1 M, pH 7.4) and stored at 4 °C.

L-cysteine-capped CdS QDs was prepared according to a published procedure.[29] Then, 0.5 mL of EGF (100 μg mL^{-1}) was added to the activated CdS QDs solution with stirring at 4 °C for 2 h. At last, the precipitum was centrifuged at 11000 rpm for 15min and then washed with deionized water. The formed CdS QDS-EGF were re-dispersed in PBS buffer (0.1 M, pH 7.4) and stored at 4 °C.

2.3. Fabrication of the sensing interface

The preparation and schematic illustration of the proposed sensing interface were displayed in Scheme 1. ITO electrode (2.0 cm × 1.0 cm) was separated into two spatially-resolved areas spaced 3 mm apart using insulation glue to avoid the cross-talk of the two areas. Subsequently, 10 mL aniline (100 μmol L^{-1}) was electro-polymerized on the two spatially-resolved areas of freshly prepared ITO electrode to form PANI/ITO with the current of 120 mA and the time of 300 s, and dried at 25 °C. Next, 20 μL AuNPs solution was coated onto the two spatially-resolved areas of PANI film respectively and dried at 25 °C for 2 h. Then, a solution containing 30 μmol L^{-1} MUC1 aptamer was dropped on the two modified areas respectively, and stored at 4 °C for 30 mins. To block possible remaining active sites, 10 μL 1% BSA was dropped on sensing interface and kept at 25 °C for 2 h. Finally, as-prepared sensing interface was cleaned with PBS buffer (0.1 M, pH 7.4). Then, the fabricated sensing interface was used for capturing MUC1-positive cell in subsequent tests.

2.4. Culturing condition of MCF-7 cells

MCF-7 cell was cultured in DMEM medium supplemented with 10% FBS and 1% antibiotics

(penicillin/streptomycin). Cell culture environment was maintained at 37°C under a humidified atmosphere containing 5% CO_2. Before measurement, MCF-7 cell was collected and separated from DMEM medium through centrifugation at 850 rpm for 5 min. These cells were then re-suspended with PBS buffer (0.1 M, pH 7.4) for the next stage of experiments.

2.5. Electrochemiluminescence detection for mannose and EGFR

MUC1 aptamer-functionalized sensing interface was incubated with cell suspension for 20 min under room temperature, followed by washing carefully with PBS buffer (0.1 M, pH 7.4) to exclude the effect of non-specific adsorption. Au@luminol-ConA and CdS QDs-EGF incubation solution were separately dropped onto the two spatially-resolved areas of sensing interface for 20 min under room temperature, respectively, as shown in Scheme 1. After that, the fabricated cytosensor was cleaned with PBS buffer (0.1 M, pH 7.4) and placed in electrochemical cell. PMT voltage was set as 750 V, and potential scanned from +0.8 V to –1.5 V in PBS buffer (0.1 M, pH 7.4) containing $K_2S_2O_8$ (0.1 M).

3. Results and discussion

3.1. Characterization of Au@luminol and CdS QDs nanoprobes

Transmission electron microscopic (TEM) was employed to characterize morphologies and sizes of the as-prepared Au@luminol and CdS QDs nanoprobes. As shown in Figure S1A, luminol coated on the surface of AuNPs to form Au@luminol nanoprobe, the average diameter of which was about 40 nm. Figure S1B displayed that the average size of CdS QDs was about 10 nm. Besides, absorption spectra of Au@luminol exhibited the absorption peak of AuNPs at 530 nm, and the absorption peaks of luminol at 300 nm and 360 nm (Figure S1C), suggested that luminol was successfully combined on the surface of AuNPs. Figure S1D exhibited that the absorption peak of CdS QDs was at 370 nm. The results showed that Au@luminol and CdS QDs nanoprobes were successfully fabricated.

3.2. Electrochemiluminescence behaviors of two potential-resolved ECL nanoprobes

The separated ECL behavior of Au@luminol or CdS QDs nanoprobes was characterized in PBS (0.1 M) solution containing $K_2S_2O_8$ (0.1 M). As shown in Figure 1A, an intense ECL signal

of CdS QDs nanoprobe was observed at –1.2 V (vs.Ag/AgCl). ECL emissions of both luminol and Au@luminol appeared at +0.5 V, but has not negative ECL in negative potential (Figure 1B). ECL intensity of Au@luminol displayed around 2.5-fold increase compared with luminol, which was due to rich luminol on the surface of AuNPs. To characterize ECL behaviors of the two nanoprobes during one potential scanning, ECL emissions of them, located on two spatially-resolved areas of a single interface, were simultaneously detected. Figure 1C showed that two potential-resolved ECL signals were obtained at the potential of +0.5 V and –1.2 V during one potential scanning, which were associated with the ECL generations of Au@luminol and CdS QDs, respectively. Therefore, the as-prepared Au@luminol and CdS QDs nanoprobes exhibited two sensitive and well-separated ECL signals at different potentials, which could act as good indicators for simultaneous detection.

3.3. Characterization of the multiplex cytosensor

The schematic diagram of fabrication process of the cytosensor was displayed in Scheme 1. Scanning electron microscopic (SEM) was employed to reveal the morphology of sensing interface. Figure 2A displayed a network structure on ITO electrode surface, this means that PANI was electropolymerized on ITO electrode and further to adsorb AuNPs (the mean diameter of AuNPs was about 40 nm, insert in Figure 2A). As shown in Figure 2B, some floccules were observed at the surface of the network structure, indicating that MUC1 aptamer was modified on AuNPs/PANI. In addition, fluorescence labeling technology was employed to conform that MCF-7 cells were captured by MUC1 aptamer on the sensing interface and the two nanoprobes were separately labeled on the cell surface, in which the green fluorescence of MCF-7 cells labeled with CdS QDs-EGF nanoprobe (Figure 2D) was stronger than that of labeled with Au@luminol-ConA nanoprobe (Figure 2C).

The stepwise fabrication process of the cytosensor was characterized through cyclic voltammetry (CV) and electrochemical impedance spectrum (EIS) measurements in PBS (0.1 M, pH 7.4) containing 5.0 mM $[Fe(CN)_6]^{4-/3-}$ and 0.1 M KCl. Figure 3A showed a pair of typical redox peaks of ferricyanide ions on bare ITO (curve a), peak current increased with the electropolymerization of PANI and the adsorption of AuNPs (curve b, c) due to excellent electric conductivity of PANI and AuNPs. After modified with MUC1 aptamer (curve d) and capturing

MCF-7 cells (curve e), peak current decreased in turn, attributing to electron inert feature of MUC1 aptamer and cells. Then, peak current decreased further after MCF-7 cells was labeled with Au@luminol-ConA and CdS QDs-EGF nanoprobes (curve f). Moreover, EIS data (Figure 3B) showed that the diameter of the semicircle decreased in turn after ITO electrode was electropolymerized with PANI and adsorbed with AuNPs (curve b, c), but increased with the modification with MUC1 aptamer, MCF-7 cells and nanoprobes (curve d, e, f). The results demonstrated that the multiplex cytosensor had successfully been fabricated.

In addition, Au@luminol-ConA and CdS QDs-EGF nanoprobes were used to recognize mannose and EGFR on MCF-7 cells, which were located on the two spatially-resolved areas of the sensing interface, respectively. The CV scan of the cell labeled with nanoprobes showed a pairs of redox peak signals coming from Au@luminol and CdS QDs (red dashed curve, Figure 3C), but no peak signal before labeled with nanoprobes (blace curve). ECL behaviors of the two nanoprobes showed two sensitive and well-separated ECL signals at +0.5 V and –1.2 V in Figure 3D (curve f). Therefore, the results confirmed that Au@luminol-ConA and CdS QDs-EGF nanoprobes successfully labeled on MCF-7 cells surface through specific binding of aptamer to ligand and showed two sensitive and well-separated ECL signals at different potentials. So, the multiplex cytosensor which could be employed to simultaneously detect mannose and EGFR at the MCF-7 cell surface during one potential scanning was successfully fabricated.

3.4. Optimization of the proposed cytosensor

To optimize detection performance of the multiplex cytosensor, several important parameters were studied. Figure S2A exhibited the effect of luminol concentration on ECL intensity of Au@luminol nanoprobe, the best concentration of luminol was 0.2 M. The maximum ECL emissions were achieved at the volume ratio of Au@luminol to ConA was 30:1 and CdS QDs to EGF was 20:1, respectively (Figure S2B and S2C). The capture time of MCF-7 cells and recognition time of Au@luminol-ConA and CdS QDs-EGF nanoprobes were further optimized to be 20 min (Figure S2D, S2E, S2F).

3.5. Evaluation of cross-reactivity

To confirm that Au@luminol-ConA and CdS QDs-EGF nanoprobes could present

well-separated ECL signals, the control tests were carried out by comparing MCF-7 cells labeled with single nanoprobe and double nanoprobes. Figure S3 showed that ECL intensity of each nanoprobe with different dosage was good agreement with that of simultaneous detection. The results indicated that the multiplex cytosensor based on a dual ECL signal system provided two sensitive and well-separated ECL signals at +0.5 V and –1.2 V and there was no energy transfer or cross reaction.

3.6. Quantitative detection of MCF-7 cells

The multiplex cytosensor was employed to quantitatively detect MCF-7 cells count by using Au@luminol-ConA and CdS QDs-EGF nanoprobes to separately label the cells on two spatially-resolved areas of a single sensing interface. The ECL intensities of both nanoprobes were proportional to the logarithms of MCF-7 cell concentrations ($100 - 1.0\times10^6$ cells mL^{-1}) in Figure 4A and 4B. With the increasing of MCF-7 cell concentration, ECL intensities of both nanoprobes increased correspondingly (Figure 4C and 4D). For Au@luminol-ConA nanoprobe, the linear regression equation was I_{ECL}=1233.1706logC_{cell} – 2041.392 with a correlation coefficient R of 0.9896 (Figure 4C). For CdS QDs-EGF nanoprobe, the linear regression equation was I_{ECL}=1463.1261logC_{cell} – 2461.692 with a correlation coefficient R of 0.9901 in Figure 4D. The detection limits of MCF-7 cells were both around 20 cells mL^{-1} (S/N=3), which were more sensitive in detecting cell amount than previous literatures.[29,35]

3.7. Quantitative evaluation of mannose and EGFR

For evaluation of the expression levels of mannose and EGFR on the surfaces of MCF-7 cells, the linear relationships between ECL intensity and cell amount, mannose expression and EGFR expression were analyzed, respectively. After incubation of the multiplex cytosensor with MCF-7 cells, the cell amount was captured by this cytosensor that could be calculated by the initial cell amount minus the remaining free cell amount in solution.[36,37] The results in Figure 5A displayed that ECL intensity for Au@luminol-ConA nanoprobe was proportional to captured MCF-7 cell amount range from 490 to 3300 cells with a correlation coefficient R of 0.9899 (n=7). The linear regression equation was as follows.

$$I_{ECL}=1.1305N - 112.546 \quad (1)$$

Meanwhile, the ECL intensity for CdS QDs-EGF nanoprobe was proportional to captured MCF-7 cell amount range from 670 to 4600 cells with a correlation coefficient R of 0.9952 (n=7), as shown in Figure 5B. The linear regression equation was as follows.

$$I_{ECL}=0.71822N + 588.983 \quad (2)$$

Further, for evaluation of the expression levels of mannose and EGFR on MCF-7 cell surface, the analysis of competitive binding was employed to block the ConA and EGF on the ECL nanoprobe surfaces by using recombinant mannose and EGFR. Mannose-blocked ConA and EGFR-blocked EGF on the two nanoprobes surfaces couldnot recognize mannose and EGFR on MCF-7 cells surface respectively, ECL intensity obtained from the cytosensor with blocked nanoprobes was lower than that from the cytosensor with non-blocked nanoprobes. Figure 5C exhibited a linear relationship between reduction value of ECL intensity ($\triangle I_{ECL}$) and recombinant mannose protein content on Au@luminol-ConA nanoprobe range from 0.1 to 1.0 pM (R=0.9924), as follows.

$$\triangle I_{ECL}=62.505C_{mannose} - 17.142 \quad (3)$$

Meanwhile, Figure 5D displayed linear relationship between reduction value of ECL intensity ($\triangle I_{ECL}$) and recombinant EGFR protein concentration on CdS QDs-EGF nanoprobe range from 0.1 to 1.0 ng mL^{-1} (R=0.9930), as follows.

$$\triangle I_{ECL}=72.067C_{EGFR} - 6.6748 \quad (4)$$

Two equations (1) and (3) were offered to calculate the mean number of mannose per MCF-7 cell, and the result was 1.2×10^6 with the relative standard deviation of 5.3 % (n=6). Moreover, the result of EGFR per MCF-7 cell was 0.86×10^5 with the relative standard deviation of 4.2 % (n=6, equations (2) and (4)). These results indicated that the dual ECL signal system was successfully fabricated and could be applied to simultaneously evaluate mannose and EGFR on the surfaces of MCF-7 cells.

3.8. Selectivity, reproducibility and stability of the multiplex cytosensor

To evaluate selectivity, reproducibility and stability, the multiplex cytosensor was investigated. MCF-7 cells with high receptors expression and human embryonic kidney (HEK) cells with low receptors expression were used to study the selectivity of the cytosensor. Figure S4A showed that two significant ECL signals were observed in the presence of MCF-7 cells, but

the signals of HEK cells were weak. Compared to MCF-7 cells, ECL intensity of the mixture of MCF-7 cells and HEK cells did not show a clear change, which exhibited that the multiplex cytosensor possessed good selectivity (Figure S4A). In addition, six ITO electrodes prepared at one time were co-cultured with MCF-7 cell suspension containing 1.0×10^3 cells mL^{-1} to illustrate reproducibility. The relative standard deviation (RSD) was 4.2 % for Au@luminol-ConA nanoprobe and 3.9 % for CdS QDs-EGF nanoprobe respectively, which indicated that the cytosensor possessed good reproducibility. The stability of the cytosensor was evaluated through continuous cyclic potential scans for 10 cycles at 1.0×10^3 cells mL^{-1} of MCF-7 cells. No obvious ECL intensity change was observed in Figure S4B. The results showed that the multiplex cytosensor had satisfying selectivity, reproducibility and stability.

4. Conclusion

In summary, an analysis platform for simultaneous evaluation of the expression levels of mannose and EGFR on the surface of MCF-7 cells was first developed by using Au@luminol-ConA and CdS QDs-EGF nanoprobes to separately label the cells on two spatially-resolved areas of a single sensing interface. The dual ECL signal system provided two well-separated and sensitive ECL signals at +0.5 V and –1.2 V during one potential scanning, respectively. The design pattern could avoid interference among different ECL probes to realize in-situ and highly sensitive detection of multiple cell-surface receptors. The strategy provided a novel platform for simultaneous evaluation of multiple cell-surface receptors and had potential application foreground in clinical analysis and disease diagnosis.

Acknowledgments

This research was financed by grants from National Natural Science Foundation of China (No. 21375048), The “Twelfth Five-Year” National Science and Technology Major Project (No. 2014ZX10003002), The Major State Basic Research Development Program of China (973 Program) (No. 2010CB833603). The authors would like to acknowledge the contribution of Zhenyou Jiang and Tao Chen to the data analyses.

Supporting Information

Characterization of Au@luminol and CdS QDs nanoprobes (Figure S1). Optimization of the proposed cytosensor (Figure S2). Evaluation of cross-reactivity (Figure S3). Selectivity, reproducibility and stability of the multiplex cytosensor (Figure S4).

References

(1) Marinissen, M. J.; Gutkind, J. S. G-Protein-Coupled Receptors and Signaling Networks: Emerging Paradigms. *Trends Pharmacol. Sci.* **2001**, *22*, 368−376.

(2) Defour, J. P.; Itaya, M.; Gryshkova, V.; Brett, I. C.; Pecquet, C.; Sato, T.; Smith, S. O.; Constantinescu, S. N. Tryptophan at the Transmembrane–Cytosolic Junction Modulates Thrombopoietin Receptor Dimerization and Activation. *Proc. Natl. Acad. Sci. U.S.A.* **2013**, *110*, 2540−2545.

(3) Snuderl, M.; Fazlollahi, L.; Le, L. P.; Nitta, M.; Zhelyazkova, B. H.; Davidson, C. J.; Akhavanfard, S.; Cahil, D. P.; Aldape, K. D.; Betensky, R. A.; Louis, D. N.; Iafrate, A. J. Mosaic Amplification of Multiple Receptor Tyrosine Kinase Genes in Glioblastoma. *Cancer Cell* **2011**, *20*, 810−817.

(4) Marth, J. D.; Grewal, P. K. Mammalian Glycosylation in Immunity. *Nat. Rev. Immunol.* **2008**, *8*, 874−887.

(5) Johns, T. G.; Mellman, I.; Cartwright, G. A.; Ritter, G.; Old, L. J.; Burgess, A. W.; Scott, A. M. The Antitumor Monoclonal Antibody 806 Recognizes a High-mannose Form of the EGF Receptor That Reaches the Cell Surface When Cells Over-express the Receptor. *FASEB J.* **2005**, *19*, 780−782.

(6) De Leoz, M. L. A.; Young, L. J. T.; An, H. J.; Kronewitter, S. R.; Kim, J.; Miyamoto, S.; Borowsky, A. D.; Chew, H. K.; Lebrilla, C. B. High-Mannose Glycans are Elevated During Breast Cancer Progression. *Mol. Cell. Proteomics* **2011**, *10*, M110.002717.

(7) Normanno, N.; De Luca, A.; Bianco, C.; Strizzi, L.; Mancino, M.; Maiello, M. R.; Carotenuto, A.; De Feo, G.; Caponigro, F.; Salomon, D.S. Epidermal Growth Factor Receptor (EGFR) Signaling in Cancer. *Gene* **2006**, *366*, 2−16.

(8) Harari, P. M. Epidermal Growth Factor Receptor Inhibition Strategies in Oncology. *Endocr. Relat. Cancer* **2004**, *11*, 689−708.

(9) Woodburn, J. R. The Epidermal Growth Factor Receptor and Its Inhibition in Cancer Therapy. *Pharmacol. Ther.* **1999**, *82*, 241−250.

(10) Guo, Z.; Hao, T.; Du, S.; Chen, B.; Wang, Z.; Li, X.; Wang, S. Multiplex Electrochemiluminescence Immunoassay of Two Tumor Markers Using Multicolor Quantum Dots as Labels and Graphene Asconductingbridge. *Biosens. Bioelectron.* **2013**, *44*, 101−107.

(11) Feng, X.; Gan, N.; Zhou, J.; Li, T.; Cao, Y.; Hu, F.; Yu, H.; Jiang, Q. A Novel Dual-Template Molecularly Imprinted Electrochemiluminescence Immunosensor Array Using $Ru(bpy)_3^{2+}$-Silica@Poly-L-lysine-Au Composite Nanoparticles as Labels For Near-Simultaneous Detection of Tumor Markers. *Electrochim. Acta* **2014**, *139*, 127−136.

(12) Wu, M. S.; Liu, Z.; Shi, H. W.; Chen, H. Y.; Xu, J. J. Visual Electrochemiluminescence Detection of Cancer Biomarkers on a Closed Bipolar Electrode Array Chip. *Anal. Chem.* **2015**, *87*, 530−537.

(13) Ida N.; Hartmann T.; Pantel J.; Schröder J.; Zerfass R.; Förstl H.; Sandbrink R.; Masters C. L.; Beyreuther K. Analysis of Heterogeneous βA4 Peptides in Human Cerebrospinal Fluid and Blood by a Newly Developed Sensitive Western Blot Assay. *J. Biol. Chem.* **1996**, *271*, 22908−22914.

(14) Elledge, R. M.; Green, S.; Pugh, R.; Allred, D. C.; Clark, G. M.; Hill, J.; Ravdin, P.; Martino, S.; Osborne, C. K. Estrogen Receptor (ER) and Progesterone Receptor (PgR), by Ligand-Binding Assay Compared With ER, PgR and pS2, by Immuno-Histochemistry in Predicting Response to Tamoxifen in Metastatic Breast Cancer: A Southwest Oncology Group Study. *Int. J. Cancer* **2000**, *89*, 111−117.

(15) Kanderova, V.; Kuzikova, D.; Stuchly, J.; Vaskova, M.; Brdicka, T.; Fiser, K.; Hrusak, O.; Lund-Johansen, F.; Kalina, T. High-Resolution Antibody Array Analysis of Childhood Acute Leukemia Cells. *Mol. Cell. Proteomics* **2016**, *15*, 1246−1261.

(16) Han, E.; Ding, L.; Jin, S.; Ju, H. Electrochemiluminescent Biosensing of Carbohydrate-Functionalized CdS Nanocomposites for in Situ Label-Free Analysis of Cell Surface Carbohydrate. *Biosens. Bioelectron.* **2011**, *26*, 2500−2505.

(17) He, Y.; Li, J.; Liu, Y. Reusable and Dual-Potential Responses Electrogenerated Chemiluminescence Biosensor for Synchronously Cytosensing and Dynamic Cell Surface N-Glycan Evaluation. *Anal. Chem.* **2015**, *87*, 9777−9785.

(18) Qiu, Y.; Wen, Q.; Zhang, L.; Yang, P. Label-Free and Dynamic Evaluation of Cell-Surface Epidermal Growth Factor Receptor Expression Via an Electrochemiluminescence Cytosensor. *Talanta* **2016**, *150*, 286−295.

(19) Wang, H.; Yuan, Y.; Chai, Y.; Yuan, R. Self-Enhanced Electrochemiluminescence Immunosensor Based on Nanowires Obtained by a Green Approach. *Biosens. Bioelectron.* **2015**, *68*, 72−77.

(20) Xu, S.; Liu, Y.; Wang, T.; Li, J. Positive Potential Operation of a Cathodic Electrogenerated Chemiluminescence Immunosensor Based on Luminol and Graphene for Cancer Biomarker Detection. *Anal. Chem.* **2011**, *83*, 3817−3823.

(21) Shang, Q.; Zhou, Z.; Shen, Y.; Zhang, Y.; Li, Y.; Liu, S.; Zhang, Y. Potential-Modulated Electrochemiluminescence of Carbon Nitride Nanosheets for Dual-Signal Sensing of Metal Ions. *ACS Appl. Mater. Interfaces* **2015**, *7*, 23672−23678.

(22) Zhou, Z.; Shang, Q.; Shen, Y.; Zhang, L.; Zhang, Y.; Lv, Y.; Li, Y.; Liu, S.; Zhang, Y. Chemically Modulated Carbon Nitride Nanosheets for Highly Selective Electrochemiluminescent Detection of Multiple Metal-ions. *Anal. Chem.* **2016**, *88*, 6004−6010.

(23) Han, F.; Jiang, H.; Fang, D.; Jiang, D. Potential-Resolved Electrochemiluminescence for Determination of Two Antigens at the Cell Surface. *Anal. Chem.* **2014**, *86*, 6896−6902.

(24) Wu, M. S.; Shi, H. W.; He, L. J.; Xu, J. J.; Chen, H. Y. Microchip Device with 64-Site Electrode Array for Multiplexed Immunoassay of Cell Surface Antigens Based on Electrochemiluminescence Resonance Energy Transfer. *Anal. Chem.* **2012**, *84*, 4207−4213.

(25) Sekar, R.B.; Periasamy, A. Fluorescence Resonance Energy Transfer (FRET) Microscopy Imaging of Live Cell Protein Localizations. *J. Cell Biol.* **2003**, *160*, 629–633.

(26) Geißler, D.; Stufler, S.; Löhmannsröben, H.-G.; Hildebrandt, N. Six-Color Time-Resolved Förster Resonance Energy Transfer for Ultrasensitive Multiplexed Biosensing. *J. Am. Chem. Soc.* **2013**, *135*, 1102–1109.

(27) Zhang, H. R.; Wu, M. S.; Xu, J. J.; Chen, H. Y. Signal-On Dual-Potential Electrochemiluminescence Based on Luminol–Gold Bifunctional Nanoparticles for Telomerase Detection. *Anal. Chem.* **2014**, *86*, 3834−3840.

(28) Liu, P. Z.; Hu, X. W.; Mao, C. J.; Niu, H. L.; Song, J. M.; Jin, B. K.; Zhang, S. Y. Electrochemiluminescence Immunosensor Based on Graphene Oxide Nanosheets/Polyaniline

Nanowires/CdSe Quantum Dots Nanocomposites for Ultrasensitive Determination of Human Interleukin-6. *Electrochim. Acta* **2013**, *113*, 176−180.

(29) Zhang, L.; Jiang, J. H.; Luo, J. J.; Zhang, L.; Cai, J. Y.; Teng, J. W.; Yang, P. H. A Label-Free Electrochemiluminescence Cytosensors for Specific Detection of Early Apoptosis. *Biosens. Bioelectron.* **2013**, *49*, 46−52.

(30) Zhang, M.; Dai, W.; Yan, M.; Ge, S.; Yu, J.; Song, X.; Xu, W. Ultrasensitive Electrochemiluminescence Immunosensor Using PtAg@carbon Nanocrystals Composites as Labels and Carbon Nanotubes-Chitosan/Gold Nanoparticles as Enhancer. *Analyst* **2012**, *137*, 2112−2118.

(31) Hua, X.; Zhou, Z.; Yuan, L.; Liu, S. Selective Collection and Detection of MCF-7 Breast Cancer Cells Using Aptamer-Functionalized Magnetic Beads and Quantum Dots Based Nano-Bio-Probes. *Anal. Chim. Acta* **2013**, *788*, 135−140.

(32) Lv, S.; Guan, Y.; Wang, D.; Du, Y. Aptamer Based Strategy for Cytosensing and Evaluation of HER-3 on the Surface of MCF-7 Cells by Using the Signal Amplification of Nucleic Acid-Functionalized Nanocrystals. *Anal. Chim. Acta* **2013**, *772*, 26−32.

(33) Cui, H.; Xu, Y.; Zhang, Z. F. Multichannel Electrochemiluminescence of Luminol in Neutral and Alkaline Aqueous Solutions on a Gold Nanoparticle Self-Assembled Electrode. *Anal. Chem.* **2004**, *76*, 4002−4010.

(34) Sakura, S. Electrochemiluminescence of Hydrogen Peroxide-Luminol at a Carbon Electrode. *Anal. Chim. Acta.* **1992**, *262*, 49−57.

(35) Su, M.; Liu, H.; Ge, L.; Wang, Y.; Ge, S.; Yu, J.; Yan, M. Aptamer-Based Electrochemiluminescent Detection of MCF-7 Cancer Cells Based on Carbon Quantum Dots Coated Mesoporous Silica Nanoparticles. *Electrochim. Acta* **2014**, *146*, 262−269.

(36) Han, E.; Ding, L.; Jin, S.; Ju, H. Electrochemiluminescent Biosensing of Carbohydrate-Functionalized CdS Nanocomposites for in Situ Label-Free Analysis of Cell Surface Carbohydrate. *Biosens. Bioelectron.* **2011**, *26*, 2500−2505.

(37) Tang, Y.; Zhang, S.; Wen, Q.; Huang, H.; Yang, P. A Sensitive Electrochemiluminescence Cytosensor for Quantitative Evaluation of Epidermal Growth Factor Receptor Expressed on Cell Surfaces. *Anal. Chim. Acta.* **2015**, *881*, 148−154.

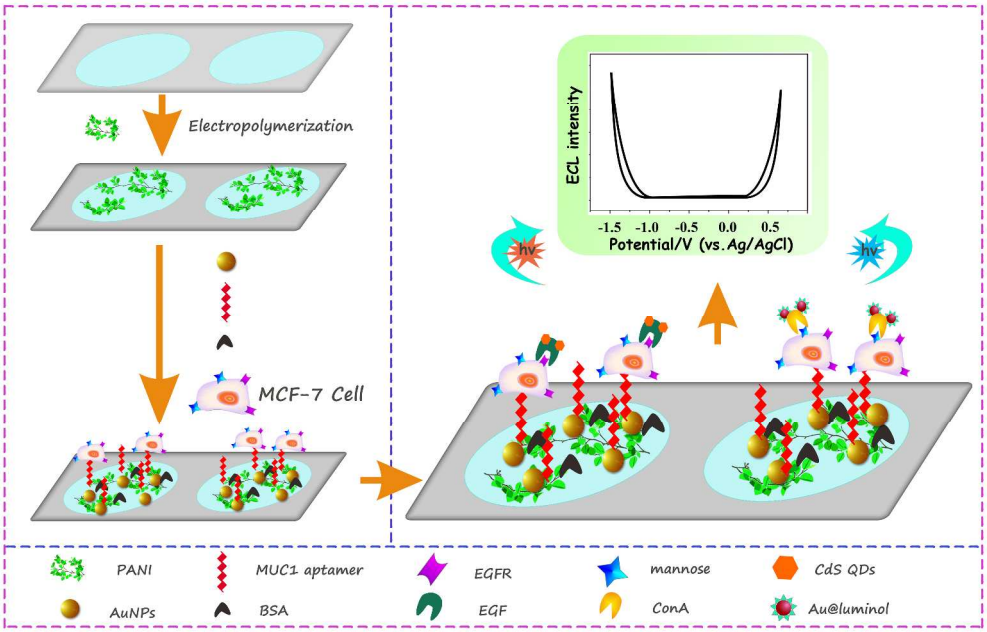

Scheme 1. Preparation and schematic illustration of the dual electrochemiluminescence signal system.
Figure captions.doc

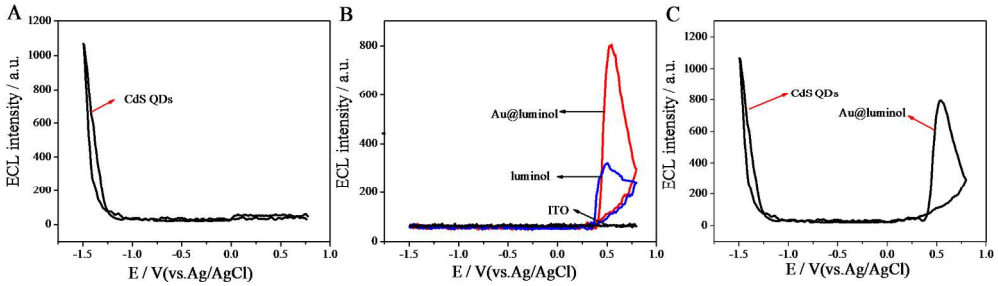

Figure 1. The ECL signal obtained on (A) CdS QDs, (B) luminol and Au@luminol, and (C) Au@luminol and CdS QDs in 0.1 M PBS (pH 7.4) containing 0.1 M K2S2O8.
Figure captions.doc

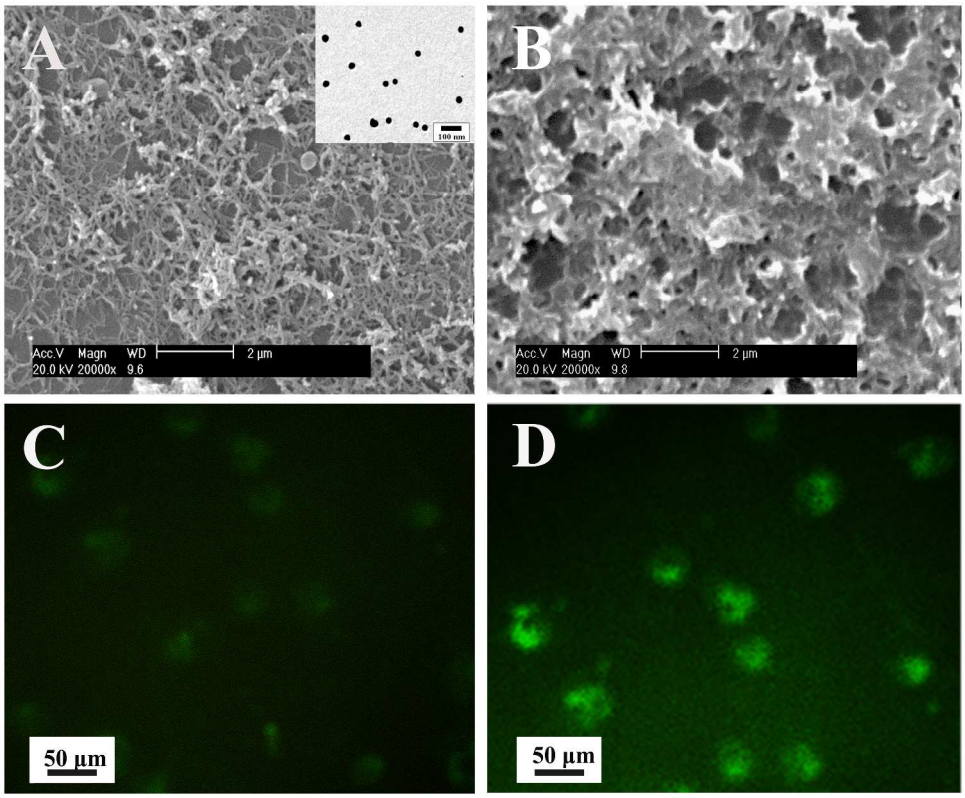

Figure 2. SEM images of (A) PANI and (B) MUC1 aptamer/AuNPs/PANI; fluorescence image of MCF-7 cells/BSA/MUC1 aptamer/AuNPs/PANI incubated with (C) Au@luminol-ConA probe, (D) CdS QDs-EGF probe. The inset of image (A) showed the TEM image of AuNPs.
Figure captions.doc

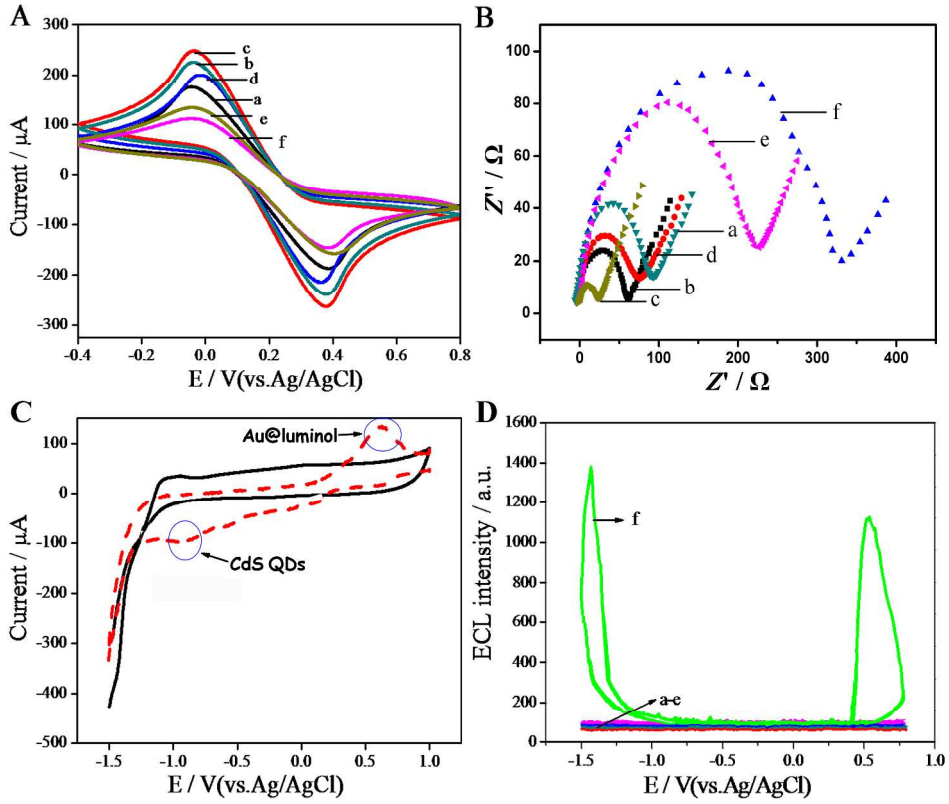

Figure 3. (A) CV responses of the different modified electrodes in 0.1 M PBS (pH 7.4) containing 5.0 mM [Fe(CN)6]4-/3- and 0.1 M KCl, (a) bare ITO, (b) PANI/ITO, (c) AuNPs/PANI/ITO, (d) BSA/MUC1 aptamer/AuNPs/PANI/ITO, (e) MCF-7 cells/BSA/MUC1 aptamer/AuNPs/PANI/ITO, (f) Au@luminol-ConA+CdS QDs-EGF probe/MCF-7 cells/BSA/MUC1 aptamer/AuNPs/PANI/ITO; (B) Electrochemical impedance spectra of the different modified electrodes in 0.1 M PBS (pH 7.4) containing 5.0 mM [Fe(CN)6]4-/3- and 0.1 M KCl, (a) bare ITO, (b) PANI/ITO, (c) AuNPs/PANI/ITO, (d) BSA/MUC1 aptamer/AuNPs/PANI/ITO, (e) MCF-7 cells/BSA/MUC1 aptamer/AuNPs/PANI/ITO, (f) Au@luminol-ConA+CdS QDs-EGF probe/MCF-7 cells/BSA/MUC1 aptamer/AuNPs/PANI/ITO; (C) CV responses of the prepared cytosensor with or without Au@luminol-ConA and CdS QDs-EGF nanoprobes in 0.1 M PBS (pH 7.4) containing 0.1 M K2S2O8; (D) ECL signal obtained on the different modified electrodes in 0.1 M PBS (pH 7.4) containing 0.1 M K2S2O8, (a) bare ITO, (b) PANI/ITO, (c) AuNPs/PANI/ITO, (d) BSA/MUC1 aptamer/AuNPs/PANI/ITO, (e) MCF-7 cells/BSA/MUC1 aptamer/AuNPs/PANI/ITO, (f) Au@luminol-ConA+CdS QDs-EGF probe/MCF-7 cells/BSA/MUC1 aptamer/AuNPs/PANI/ITO.
Figure captions.doc

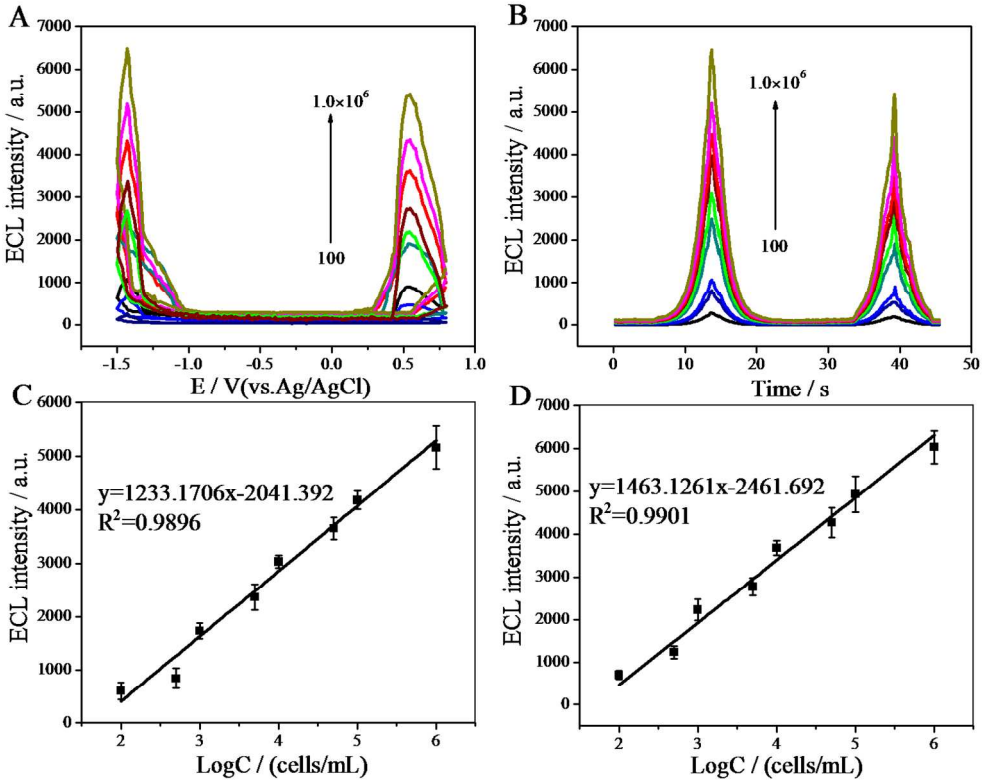

Figure 4. (A) and (B) ECL signal obtained on Au@luminol-ConA and CdS QDs-EGF nanoprobes with MCF-7 cell concentrations of 100, 500, 1.0 × 103, 0.5 × 104, 1.0 × 104, 0.5 × 105, 1.0 × 105, 1.0 × 106 cells mL-1; linear relationship between logarithm of MCF-7 cell concentrations and ECL intensity of (C) Au@luminol-ConA, (D) CdS QDs-EGF.
Figure captions.doc

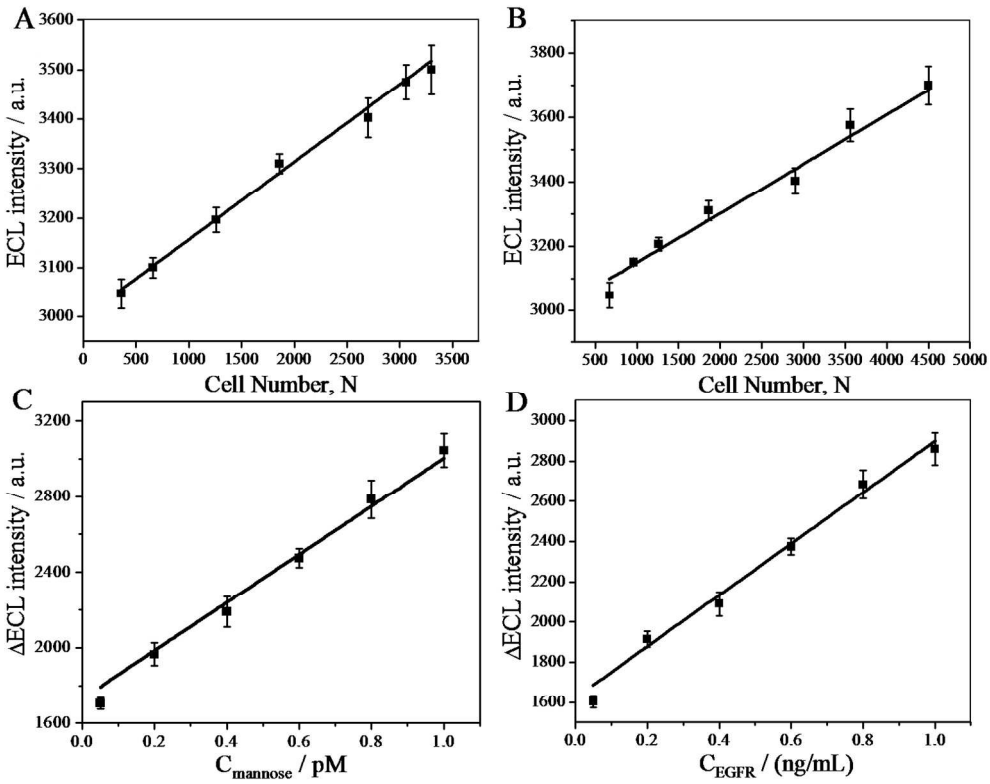

Figure 5. Linear relationship between number of captured MCF-7 cells on the cytosensor and ECL intensity of (A) Au@luminol-ConA, (B) CdS QDs-EGF; effect of (C) the recombinant mannose concentration and (D) the recombinant EGFR concentration on the reduction value of ECL intensity.
Figure captions.doc

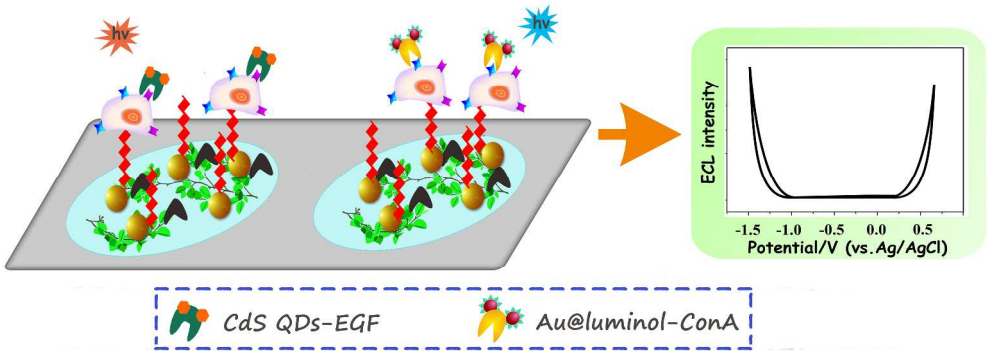

Graphical Abstract